

Role of Siloxy Substituents in the Activation of Zirconocene Polymerization Catalysts with Methylaluminoxane. A Combined Spectroscopic and Theoretical Study

Nora I. Mäkelä-Vaarne*,†

Borealis Polymers Oy, R&D, P.O. Box 330, FIN-06101 Porvoo, Finland

Mikko Linnolahti* and Tapani A. Pakkanen

Department of Chemistry, University of Joensuu, P.O. Box 111, FIN-80101 Joensuu, Finland

Markku A. Leskelä

Department of Chemistry, University of Helsinki, P.O. Box 55, FIN-00014 University of Helsinki, Finland

Received January 28, 2003; Revised Manuscript Received March 20, 2003

ABSTRACT: The activation of 1-siloxy-substituted zirconocene with MAO occurs slowly, in 4–6 h. The slow activation process involves three distinct ligand to metal charge transfer (LMCT) band shifts in the UV/vis spectrum before the maximum LMCT absorption energy and intensity of the third appearing band is reached. In addition, at very high MAO concentrations, a fourth band at 460 nm begins to form. On the contrary, the corresponding 2-siloxy-substituted as well as the unsubstituted zirconocene react with MAO in less than a minute, immediately producing the final species, as confirmed by only one observed LMCT band shift. The 1-silyl-substituted zirconocene reacts with MAO, producing the final active species in 1 h. UV/vis spectroscopic observations were interpreted with the aid of molecular modeling studies, demonstrating that the interactions of the oxygen donor atom of the siloxy substituent with electron deficient Zr center and coordinatively unsaturated Al in MAO play a prominent role in the activation process.

Introduction

Catalysts based on metallocene complexes exhibit high olefin polymerization activities when activated with methylaluminoxane (MAO).¹ The single-site nature of metallocene catalysts enables the synthesis of polymers with narrow molecular weight distributions and tailored microstructures. This is a significant advantage compared to conventional industrially utilized heterogeneous Ziegler–Natta catalysts, containing several different active sites. Notwithstanding the benefits of single-site metallocene catalysts, the factors controlling polymerization behavior have not been fully solved. Generally, electron-donating substituents on the ligand framework are supposed to increase the catalytic activity, which is due to stabilization of the active cationic species. The influence of electron-withdrawing substituents is reverse, complicating the activation of the catalyst precursor.²

When attached to the ligand framework of zirconocene catalyst, siloxy groups act as electron donors.³ The catalysts exhibit higher activities than their unsubstituted congeners, especially at low [Al]/[Zr] ratios.⁴ In certain cases, the catalytic activity decreases with increasing [Al]/[Zr] molar ratio and also long induction times have been reported.⁵ It is notable, that the activity of the corresponding oxygenless silyl-substituted zirconocene is much lower.⁶ This is somewhat surprising, since the capabilities of the two electron-donating substituents in stabilizing the active cationic species are roughly equal.²

The present study was motivated by the significant differences in the catalytic performance of siloxy- and silyl-substituted zirconocene catalyst, when activated with MAO. The paper aims at clarifying the role of siloxy-substituent in the activation process by combining UV/vis and ²⁹Si NMR spectroscopic observations with molecular modeling studies.

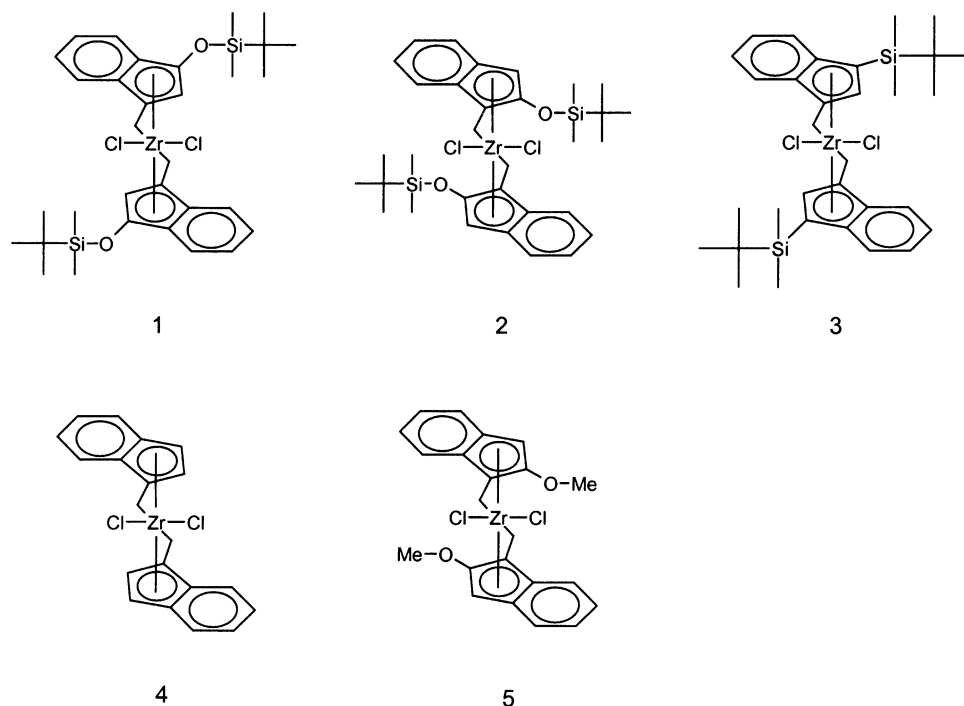
Experimental Section

Siloxy- and silyl-substituted zirconocenes (Scheme 1) were synthesized and characterized by Leino⁷ and Ekholm.⁸ Complex **4** was purchased from Witco. Preparation of dimethylated form of complex **2** is described in ref 15. Methylaluminoxane (MAO 30 wt % in toluene) was purchased from Albemarle and stored in a freezer. The trimethylaluminum (TMA) content of MAO was given to be 4.9 wt %.

UV/vis Spectroscopy. For the UV/vis measurements, a metallocene–toluene solution (8×10^{-4} mol/L Zr) was transferred to a 1 cm path length quartz cell equipped with Teflon stoppers. The samples were analyzed using Perkin-Elmer Lambda 900 spectrophotometer. Optionally MAO, [Al]/[Zr] = 1700, 2500, 5000, and 7500 and for complexes **1**, **2**, and **4** also 15 000, was injected to the measurement cells and the reactions were followed by scanning the UV/vis spectrum with 1 min intervals for the first 30 min and after this hourly up to 7 h and once after 24 h. All measurements were performed under inert conditions using dried toluene and at room temperature.

²⁹Si NMR Spectroscopy. The dimethyl form of complex **2**/toluene/deuteriobenzene solution with 10 wt % of zirconocene and approximately 10% of deuteriobenzene was analyzed with ²⁹Si NMR spectroscopy. Trimethylaluminum, [Al]/[Zr] = 20, was added to this mixture and the ²⁹Si NMR spectrum was scanned again. The spectra were run on a CMX Infinity 400 NMR spectrometer at room temperature. The chemical shifts were referenced to tetramethylsilane.

† E-mail: nora.makela-vaarne@borealisgroup.com.

Scheme 1. Schematic Structures of the Studied Zirconocenes in the Dichloride Precursor Form

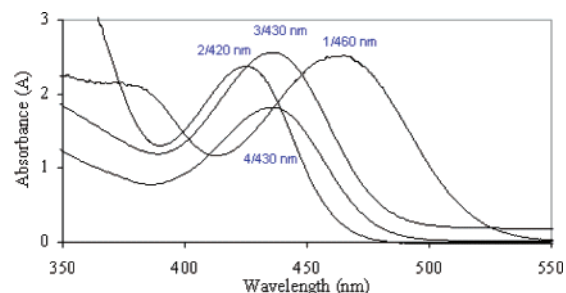
^a Key: (1) *rac*-(ethylenebis(1-*tert*-butyldimethylsiloxy)indenyl)zirconium dichloride; (2) *rac*-(ethylenebis(2-*tert*-butyldimethylsiloxy)indenyl)zirconium dichloride; (3) *rac*-(ethylenebis(1-*tert*-butyldimethylsilyl)indenyl)zirconium dichloride; (4) *rac*-(ethylenebis(indenyl))zirconium dichloride; (5) *rac*-(ethylenebis(2-methoxy)indenyl)zirconium dichloride (included only in the modeling studies).

Theoretical Calculations. All calculations were performed by the Hartree–Fock method with a standard 3-21G* basis set. The HF/3-21G* method produces accurate structures for zirconocenes, as demonstrated by a recent comparison between optimized and experimentally determined crystal structures of 62 bridged zirconocene dichlorides.⁸ The accuracy of the geometry predictions was practically equal to the more sophisticated B3LYP and MP2 methods. The success of the HF/3-21G* method for zirconocenes originates from insignificant near-degeneracy correlation⁹ and relativistic effects,¹⁰ which are major factors contributing to the troublesome treating of transition metal complexes in general.¹¹ Calculations were carried out with Gaussian 98 quantum chemical software.¹²

Results and Discussion

The studied zirconocene catalysts are presented in Scheme 1. Representative 1-siloxy- (**1**) and 2-siloxy-substituted (**2**) zirconocenes were selected for the study to investigate the effect of the position of the siloxy substituent on the activation process. To elucidate the impact of the oxygen atom on the activation, the corresponding oxygenless 1-silyl-substituted zirconocene¹³ (**3**) was studied as well, while the unsubstituted complex (**4**) was included as a reference. Furthermore, a 2-methoxy-substituted zirconocene (**5**) was incorporated in the modeling studies.

The ligand to metal charge transfer (LMCT) absorption bands of zirconocene precursors and zirconocenes activated with MAO were detected by UV/vis spectroscopy. The energies of the absorptions provide useful information on the electronic properties of metallocene complexes^{3,14} and can be utilized to study the activation process.^{15,16} The lowest energy LMCT absorption occurs due to the charge transfer from the electron-rich Cp-based ligand (Cp') to the electron poor metal center. Methylation of the zirconocene dichloride by low concentrations of MAO results in a LMCT band shift to

**Figure 1.** LMCT absorptions of the studied zirconocene complexes in toluene.

higher energies, i.e. to shorter wavelengths. The replacement of chlorines with more electron-donating methyl groups increases the electron density at the metal. Consequently, additional energy is required to move electron density from Cp' to Zr. Methylation was not observed in this study since we used sufficiently high [Al]/[Zr] ratios to result in zirconocene cationization. Methylation of these zirconocenes has been studied before.¹⁵ The formation of a cationic zirconocene shifts the LMCT band to lower energy. The electron density at the central metal decreases due to the loss of chlorine or methyl ligand, resulting in a more facile Cp' → Zr charge transfer.^{14,15}

Catalyst Activation. The LMCT absorptions of zirconocene complexes in toluene are presented in Figure 1. The absorption energy is clearly lower for the 1-siloxy-substituted complex **1** than for its 1-silyl-substituted congener (**3**), which absorbs at the same energy of 430 nm with the unsubstituted catalyst precursor. This change, however, does not allow us to determine the electronic character of the substituents, since the geometries of the compounds have a notable influence on the LMCT absorption energies as well.^{3,14} Generally, increasing Cp'–Cp' and Cp'–Zr–Cp' angles

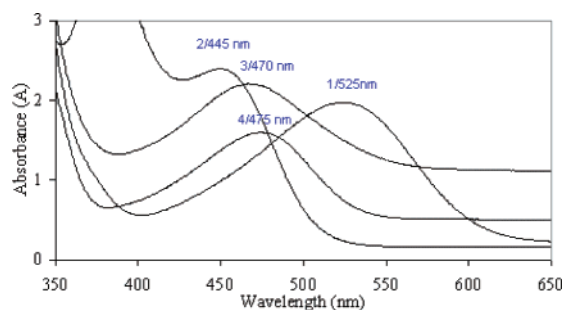


Figure 2. LMCT absorptions of the final active forms of the studied zirconocenes activated with MAO. $[Al]/[Zr] = 2500$, reaction time 6 h.

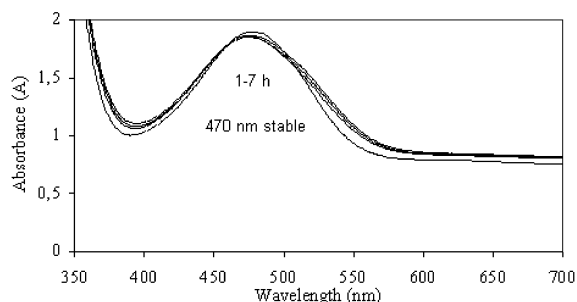
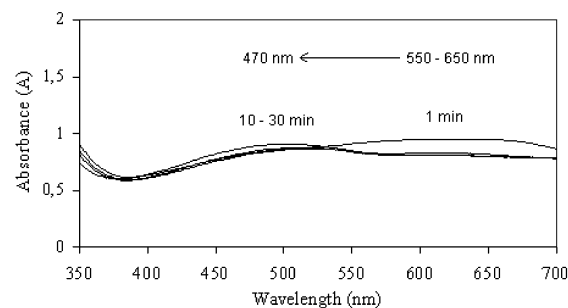


Figure 3. UV-vis spectra of complex **3** with MAO $[Al]/[Zr] = 1700$. The reaction was monitored from the first minute up to 7 h.

decrease the LMCT energy³ as well as moving toward the backward orientation.¹⁴ The lowered LMCT energy arises due to the distortion of the complex geometry from optimal bonding between Zr and Cp'. Structural changes are a major contributor to the increase of 40 nm in the absorption energy when moving from the 1-siloxy-substituted (**1**) to the 2-siloxy-substituted (**2**) zirconocene dichloride.³

The spectra of the final active forms of the studied zirconocenes activated with MAO, $[Al]/[Zr] = 2500$, are shown in Figure 2. The spectra of 1-silyl-substituted (**3**) and unsubstituted (**4**) species are similar, whereas the siloxy-substituted catalysts absorb at lower (**1**) and higher (**2**) energies. Again, due to the contribution of structural factors, we cannot draw conclusions of differences in the active sites. Therefore, we decided to study the activation behavior, i.e. what happened on the way to the final active forms of the catalyst as a function of time and MAO concentration.

Activation Behavior. The UV-vis spectra as a function of time for 1-silyl- (**3**) and 1-siloxy-substituted (**1**) complexes reacted with $[Al]/[Zr] = 1700$ concentration of MAO are shown in Figures 3 and 4, respectively. The differences in the activation behavior are evident. For complex **1**, three distinct reaction time dependent

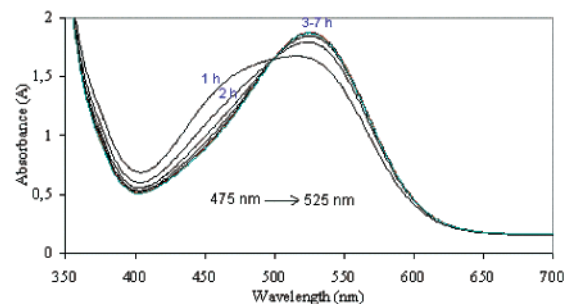
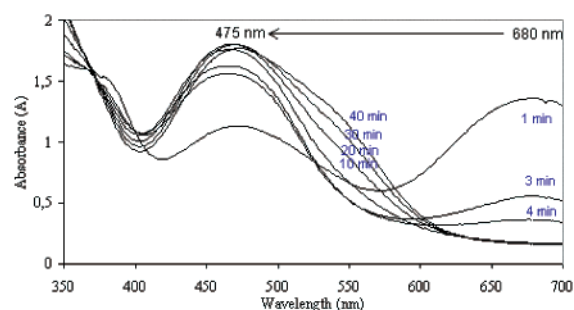


Figure 4. UV-vis spectra of complex **1** with MAO $[Al]/[Zr] = 1700$. The reaction was monitored from the first minute up to 7 h.

catalyst intermediate species were observed, while only one intermediate was observed for complex **3**. Initially, the silyl-substituted catalyst **3**, when activated with MAO, had a hardly discernible absorption band maximum in the range 550–650 nm (Figure 3). Another absorption band started to form after approximately 10 min at 470 nm, accompanying the disappearance of 550–650 nm absorption band. This band was fully formed in an hour and it represents the absorption maximum of the final active species. Similar behavior was observed at $[Al]/[Zr]$ molar ratios of 2500, 5000, and 7500. The 470 nm band was stable for at least 24 h.

For the siloxy-substituted complex **1** activated with MAO, the first absorption band formed at approximately 680 nm, and disappeared in 5 min independently on the $[Al]/[Zr]$ ratio. Simultaneously, a band at 475 nm started to form and reached its maximum in 10 min, again independent of the $[Al]/[Zr]$ ratio. This band disappeared in 3–6 h. The disappearance took a longer time with increasing $[Al]/[Zr]$ ratio. After 1 h, a band at 525 nm appeared and increased constantly up to 4–6 h. The maximum absorbance of this final band was achieved slower with higher $[Al]/[Zr]$ ratios. The 525 nm band was stable for more than 24 h at $[Al]/[Zr]$ ratios of 1700, 2500, and 5000 indicating that the intermediate species absorbing at 475 nm are slowly transforming into the species absorbing at 525 nm and that the reaction kinetics is dependent on the concentration of MAO.

The active species of the 1-siloxy-substituted complex **1** + MAO ($[Al]/[Zr] = 1700, 2500$, or 5000) absorbs at 525 nm, as described earlier. However, at even higher $[Al]/[Zr]$ ratios of 7500 and 15 000, a new shoulder begins to form at around 460 nm (Figure 5). This behavior was detected for complex **1** only. The ratio of the 460 nm band and the 525 nm band, $A(460\text{ nm})/A(525\text{ nm})$, increases with increasing MAO concentrations.

The unsubstituted complex (**4**) and 2-siloxy-substituted complex (**2**) activated with variable MAO concentrations ($[Al]/[Zr] = 1700\text{--}15\,000$) absorb at 475 and 445

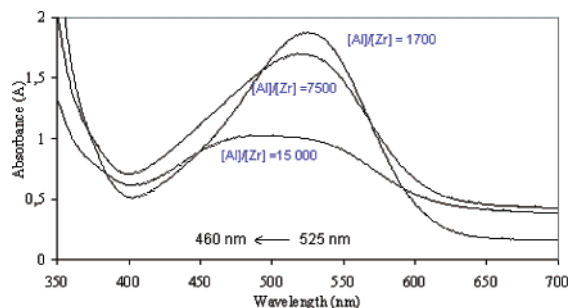


Figure 5. UV-vis spectra of complex **1** with MAO $[Al]/[Zr]$ = 1700, 7500, and 15 000 after reaction time of 6 h.

nm, respectively. The absorptions are formed in less than a minute, and are stable for more than 24 h.

Discussion of the Activation Behavior. When reacted with MAO, the 1-silyl-substituted complex (**3**) absorbs weakly at around 550–650 nm during the first 10 min. We tentatively assign this as a transition-state of activation. After this, the absorption maximum at 470 nm, representing the final active species, was fully formed in 1 h. The activation of 1-silyl-substituted catalyst (**3**) takes much longer time than the activation of the unsubstituted catalyst (**4**), for which the final absorption band position and intensity was reached in less than a minute. This is probably due to the bulky silyl substituent, which hinders the access of MAO to the metal center.

The differences in the activation behavior of the 1-siloxy (**1**) and 2-siloxy (**2**) substituted complexes reacted with MAO are notable—the final form of complex **2** reaches the maximum concentration faster, in 1 min, than complex **1**, for which it takes four to 6 h depending on MAO concentration. Corresponding behavior has been observed in olefin polymerization studies: clearly a longer induction period was observed for 1-siloxy-substituted complex (**1**) than for its 2-siloxy-substituted congener (**2**).⁵ Induction times of several hours have also been observed earlier by Brintzinger et al. for a 2-(dimethylamino)-substituted bis(indenyl) *ansa*-zirconocene/MAO catalyst system in propylene polymerization.¹⁷ The activation of 1-siloxy-substituted complex (**1**) occurs in three steps. It has been observed that the activity of complex **1** is decreased and induction times for activation prolonged with increasing MAO concentration.⁵ Since the formation of the third band at 525 nm was $[MAO]$ -dependent, so that the formation was slower at higher MAO concentrations, we conclude that this band is the LMCT of the most active form of the complex **1**–MAO. The second band at 475 nm can be the cationic form of complex **1**, which involves siloxy coordination to some other catalyst fragments, e.g. electron deficient Zr center. The first appearing band of complex **1**–MAO at 680 nm could be a transition state of activation, as suggested also for complex **3**.

A shoulder at 460 nm, which was observed only for complex **1** at high $[Al]/[Zr]$ ratios of 7500 and 15 000, suggests that complex **1** has an additional interaction with MAO. This interaction is more pronounced at higher $[Al]/[Zr]$ ratios. The consequence of the interaction would be an inductive electron withdrawal, destabilizing the active cationic species and therefore leading to decreased polymerization activity observed at high $[Al]/[Zr]$ ratios.⁵

Activation of the 2-siloxy-substituted complex (**2**) does not involve three time-consuming reaction steps, as is the case with the 1-siloxy-substituted complex (**1**). The

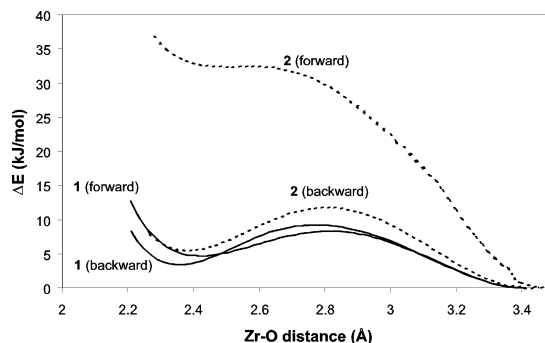


Figure 6. Energetics of Zr–O(siloxy) interaction as a function of Zr–O(siloxy) distance for siloxy-substituted complexes **1** (dashed line) and **2** (solid line) in cationic monomethyl form.

prolonged induction period in olefin polymerization with increasing $[Al]/[Zr]$ molar ratio, which has been observed for the 1-siloxy-substituted complex (**1**), was not recorded for its 2-siloxy-substituted congener (**2**).⁵ Taking this into account, the different behavior of siloxy-substituted zirconocenes compared to silyl- or unsubstituted ones may not arise alone from the coordination of siloxy oxygen to Al of MAO, as proposed earlier.^{5,18} To further clarify the role of the siloxy substituent, we conducted molecular modeling studies on Zr–O(siloxy) and (MAO)Al–O(siloxy) interactions. The electron-deficient metal center (Zr), as well as the Lewis-acidic Al in MAO, is most prone to interact with electron-rich oxygen in the siloxy substituent.

Zr–O(siloxy) Interaction. The possible interaction between the cationic metal center and the oxygen donor atom of the siloxy group was studied by systematically shortening the O–Zr distance in cationic monomethyl forms of siloxy-substituted zirconocenes. It is notable that the complexes favor two distinct conformations originating from the flexibility of the ethylene bridge, indenyl-forward and indenyl-backward, which are both present in the solution due to a low interconversion barrier of approximately 20 kJ/mol.¹⁹ While indenyl-forward conformations are generally favored, 2-siloxy-substituted complexes slightly prefer the indenyl-backward conformation.²⁰ The Zr–O(siloxy) interactions were studied for both conformations and the results are presented in Figure 6. The interaction is very facile for both backward and forward conformations of complex **1**, with barriers of less than 10 kJ/mol. For complex **2**, instead, the capability of forming an interaction between Zr and O is strongly dependent on the conformation. The interaction is favorable for the backward conformation while it is strongly unfavorable for the forward conformation. This difference is due to the fact that complex **2**, when oriented in the forward conformation, has its siloxy group pushed backward, toward the ethylene bridge. Hence, the oxygen atom cannot reach the metal center without destabilizing distortions in the molecular structure.

Overall, the Zr–O(siloxy) interaction, which is stronger for the 1-siloxy-substituted than for the 2-siloxy-substituted complex, may be a reason for the longer induction periods observed for 1-siloxy-substituted zirconocene (**1**) than for its 2-siloxy- (**2**), 1-silyl- (**3**), and unsubstituted (**4**) congeners.^{4,5,6} While resulting in a prolonged catalyst activation step, the Zr–O(siloxy) interaction may also contribute to the highest polymerization activity of this catalyst series observed for **1**,^{5,6} owing to stabilization of the intermediate as well as the activated species. Apparently, the Zr–O(siloxy)

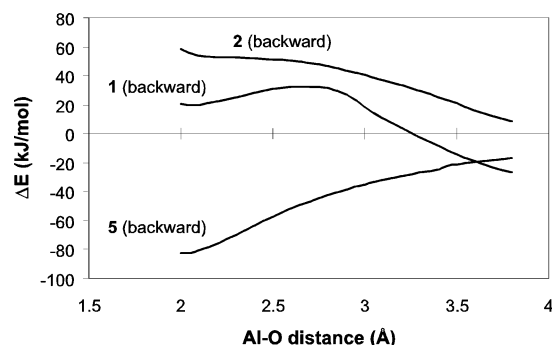


Figure 7. Energetics of Al(TMA)–O(siloxy or methoxy) interaction for complexes **1**, **2** and **5** + TMA. The energies are given relative to the sum of free species (TMA + complex).

interaction is present at variable extents throughout the catalyst activation steps.

(MAO)Al–O(siloxy) Interaction. Earlier work of Piccolrovazzi et al.¹⁸ has demonstrated that the modest activity of methoxy-substituted zirconocenes is due to coordination of Lewis-acidic aluminum to the oxygen donor atom of the methoxy group. The resulting inductive electron withdrawal destabilizes the active species, leading to a decrease in polymerization activity due to the unavailability of the active reaction centers for olefins to react with. On the contrary, siloxy-substituted zirconocenes show markedly higher polymerization activities, even higher than those of silyl-substituted catalysts.⁶ Apparently, the high activities at low activator concentrations are due to the bulkiness of the siloxy group, hindering the (MAO)Al–O(siloxy) interaction.²

To confirm the suggestion, we performed molecular modeling studies on the interaction between the Lewis-acidic aluminum of TMA and the oxygen donor atoms of methoxy- (**5**) and siloxy-substituted (**1** and **2**) catalyst precursors in the preferred backward conformation. Since the focus is on the interaction between the substituent and the coordinatively unsaturated, Lewis-acidic aluminum center of the activator, three-coordinated TMA can be considered as a sufficient model for qualitative purposes. The energetics of the interactions are presented in Figure 7 as a function of the (MAO)–Al–O(siloxy or methoxy) distance. For methoxy-substituted complex **5**, which has a poor activity, the (MAO)–Al–O(methoxy) interaction is spontaneous, whereas the bulky siloxy-substituents are capable of blocking TMA thus making the (MAO)Al–O(siloxy) interaction unfavorable. The blocking is more efficient with the 2-siloxy-substituent. In the case of complex **1**, the interaction is favorable compared to the sum of free species at (MAO)–Al–O(siloxy) distances of longer than 3.3 Å. This is due to the electron deficient AlMe₃, interacting with other electron-rich portions of the catalyst precursor. AlMe₃ is not stable as such but tends to dimerize to Al₂Me₆.

The activity of complex **1**–MAO decreases with increasing MAO concentration (constant complex–MAO pre-contact time) while the activity of complex **2**–MAO is not significantly affected.⁵ Modeling studies support these observations, suggesting that when Al atoms are present in very high concentrations they can penetrate through the bulky siloxy group, eventually leading to the unfavorable (MAO)Al–O(siloxy) interaction. As shown in Figure 7, the shielding of the oxygen donor atom is more efficient with 2-siloxy-substituent. Consequently, it is also less sensitive to MAO concentrations—even [Al]/[Zr] ratios of 15 000 did not affect the

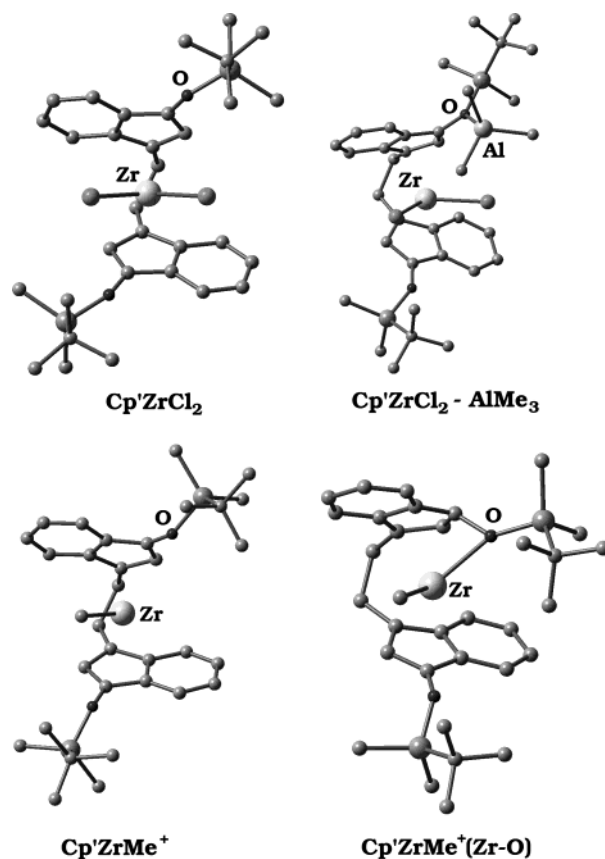


Figure 8. Optimized structures for the studied catalyst intermediates of complex **1**. Hydrogens are omitted for clarity.

Table 1. Calculated Orbital Energies (eV) of the Different Species of the 1-Siloxy-Substituted Complex (**1**)

	Cp' ₂ ZrCl ₂	Cp' ₂ ZrCl ₂ –AlMe ₃	Cp' ₂ ZrMe ⁺	Cp' ₂ ZrMe ⁺ (Zr–O(siloxy))
HOMO	–7.15	–7.55	–10.41	–10.18
LUMO	1.14	0.94	–2.37	–1.48
LUMO–HOMO	8.30	8.49	8.04	8.70

wavelength of the formed absorption at 445 nm in the UV/vis spectrum. The 1-siloxy-substituted catalyst (**1**) is more easily affected by the (MAO)Al–O(siloxy) interaction, resulting in the observed decrease in polymerization activity with increasing MAO concentration.

Optimized structures of the studied catalyst species of complex **1** are presented in Figure 8. Since the lowest energy LMCT absorptions are due to charge transfer from the Cp' ligand (HOMO) to the metal center (LUMO),³ the absorption energies of the intermediates can be predicted by considering the LUMO–HOMO energy gaps (Table 1).

Cationization of the catalyst precursor considerably stabilizes both HOMO and LUMO. The stabilization is more pronounced for LUMO, decreasing the HOMO–LUMO energy gap, and consequently the LMCT absorption energy. The Al(MAO)–O(siloxy) coordination mostly affects the HOMO orbital which is stabilized from –7.15 to –7.55 eV due to the inductive electron withdrawal from the Cp' ligand. The simultaneous stabilization of LUMO orbital from 1.14 to 0.94 eV is less significant. Consequently, the LUMO–HOMO energy gap, and hence the LMCT absorption energies, increase. The coordination of the siloxy oxygen to the cationic metal center considerably destabilizes the LUMO orbital, therefore increasing both LUMO–HOMO energy gaps and LMCT absorption energies.

The increases in the HOMO–LUMO energy gaps with the Al(MAO)–O(siloxy) or Zr–O(siloxy) interactions suggest that the absorption bands, which are due to the species having these interactions, should be located at higher energy than those without such interactions. This agrees qualitatively to the spectral shifts observed for catalyst **1**. The formation of the active species, which absorbs at 525 nm, is preceded by higher energy band at 475 nm. Apparently, this band at 475 nm, which was detected only for the 1-siloxy-substituted catalyst, arises from the presence of an intermediate involving a strong Zr–O(siloxy) interaction. The Zr–O(siloxy) interaction loosens up with the increasing reaction time of metallocene-MAO system. The formation of Al(MAO)–O(siloxy) interaction requires a higher concentration of MAO—it can be seen at [Al]/[Zr] = 7500 and 15 000 for complex **1** (Figure 5), when a new shoulder at 460 nm begins to form. With high Al(MAO) concentrations the Al(MAO)–O(siloxy) interaction becomes relevant, resulting in inductive electron withdrawal from the Cp' ligand to Al(MAO) and thus in the observed increase of the Cp' → Zr CT energy.

The interaction between aluminalkyls and the siloxy-substituent was also studied with ^{29}Si NMR. To prevent the interference of chemical shifts caused by the reaction between aluminalkyl and zirconocene dichloride, i.e. chloride–methyl transfer, we concentrated on the dimethylated form of the catalyst. The reaction between the dimethylated 2-siloxy-substituted catalyst (**2**-Me₂) and trimethylaluminum (TMA) was considered. TMA was applied instead of MAO since, unlike MAO, it is known only to methylate the complex, i.e., the observed changes in the Si chemical shifts will arise from the siloxy substituent interactions only and not, e.g., on zirconocene cationization. Surprisingly, no differences in the chemical shifts were observed between the dimethylated form of complex **2** and the same complex reacted with TMA ([Al]/[Zr] = 20). The silicons of both samples were observed at 49 ppm, indicating that the siloxy substituent does not interact with the Lewis-acidic aluminum of TMA at these low concentrations. Apparently, the use of TMA alone cannot explain the function of MAO, but it gives supporting indications for the UV/vis studies involving MAO.

Conclusions

The studied siloxy-, silyl-, methoxy-, and unsubstituted *rac*-(ethylenebis(indenyl))zirconium dichlorides possess clearly dissimilar catalytic properties in olefin polymerization. The LMCT absorptions of metallocenes detected using UV/vis spectroscopy are sensitive toward changes in the complex geometry. Conclusions on the differences in the active species derived from different metallocene complexes and MAO can be drawn only if the metallocene complex structures are very uniform, which was not the case in this study. Therefore, we decided to study the activation kinetics of a group of metallocenes.

Combined UV/vis spectroscopic and molecular modeling studies suggest that the Zr–O(siloxy) interaction is the reason for the observed long induction period in olefin polymerization recorded for 1-siloxy-substituted zirconocene (**1**). This is supported by the calculated feasibility of Zr–O(siloxy) interaction and slow formation of the active species, 4–6 h, recorded by UV/vis spectroscopy. The Zr–O(siloxy) interaction was less significant for the corresponding 2-siloxy-substituted

catalyst (**2**), for which long induction times has not been observed. According to UV/vis spectroscopy, the final species of complex **2**/MAO is formed in less than 1 min.

UV/vis spectroscopic studies suggested that (MAO)–Al–O(siloxy) interaction, earlier demonstrated for corresponding methoxy-substituted catalysts, was present only at high [Al]/[Zr] ratios, i.e., >7500. ^{29}Si NMR spectroscopy did not either show the presence of (TMA)–Al–O(siloxy) interaction at low TMA/metallocene ratios, i.e., [Al]/[Zr] = 20. When MAO is present at high concentrations, the coordinatively unsaturated Al may interact with the oxygen donor atom of the siloxy substituent, resulting in destabilization of the active species due to inductive electron withdrawal from (siloxy)O to coordinatively unsaturated Al in MAO and leading to a decrease in polymerization activity. As shown by the calculations, the (MAO)Al–O(siloxy) interaction is more significant for the 1-siloxy-substituted zirconocene (**1**), for which also a clear decrease in polymerization activity with increasing MAO concentration has been observed.

Acknowledgment. Dr. Taito Väänänen (Fortum Oil & Gas OY) is thanked for the NMR and Ms. Paula Oinonen for the UV/vis spectroscopic measurements. The previous work by and discussions with Dr. Petri Lehmus and Dr. Peter Ekholm are acknowledged. We would like to express our thanks for the financial support from the Academy of Finland.

References and Notes

- (1) See, for example, the following reviews and references therein: (a) Möhring, P. C.; Coville, N. J. *J. Organomet. Chem.* **1994**, 479, 1. (b) Brintzinger, H. H.; Fischer, D.; Mühlaupt, R.; Rieger, B.; Waymouth, R. M. *Angew. Chem., Int. Ed. Engl.* **1995**, 34, 1143. (c) Kaminsky, W. *Macromol. Chem. Phys.* **1996**, 197, 3907. (d) Kaminsky, W.; Arndt, M. *Adv. Polym. Sci.* **1997**, 127, 143. (e) Janiak, C. In *Metallocenes: Synthesis, reactivity, applications*; Togni, A., Halterman, R. L., Eds.; Wiley-VCH: Weinheim, Germany, 1998. (f) Hlatky, G. G. *Chem. Rev.* **2000**, 100, 1347.
- (2) Linnolahti, M.; Pakkanen, T. A. *Macromolecules* **2000**, 33, 9205.
- (3) Mäkelä, N. I.; Knuuttila, H. R.; Linnolahti, M.; Pakkanen, T. A. *J. Chem. Soc., Dalton Trans.* **2001**, 1, 91.
- (4) Leino, R.; Luttikhedde, H. J. G.; Lehmus, P.; Wilén, C.; Sjöholm, R.; Lehtonen, A.; Seppälä, J. V.; Näsman, J. H. *Macromolecules* **1997**, 30, 3477.
- (5) Lehmus, P.; Kokko, E.; Härkki, O.; Leino, R.; Luttikhedde, H.; Näsman, J. H.; Seppälä, J. *Macromolecules* **1999**, 32, 3547.
- (6) Ekholm, P.; Lehmus, P.; Kokko, E.; Haukka, M.; Seppälä, J.; Wilén, C.-E. *J. Polym. Sci., Part A: Polym. Chem.* **2001**, 39, 127.
- (7) (a) Leino, R.; Luttikhedde, H.; Wilén, C.-E.; Sillanpää, R.; Näsman, J. H. *Organometallics* **1996**, 15, 2450. (b) Leino, R.; Luttikhedde, H. J. G.; Lehtonen, A.; Ekholm, P.; Näsman, J. H. *J. Organomet. Chem.* **1998**, 558, 181.
- (8) Linnolahti, M.; Hirva, P.; Pakkanen, T. A. *J. Comput. Chem.* **2001**, 22, 51.
- (9) Siegbahn, P. E. M. *Adv. Chem. Phys.* **1996**, 93, 333.
- (10) Pyykkö, P. *Chem. Rev.* **1988**, 88, 563.
- (11) Veillard, A. *Chem. Rev.* **1991**, 91, 743.
- (12) Gaussian 98, Revision A.11.3, Frisch, M. J.; Trucks, G. W.; Schlegel, H. B.; Scuseria, G. E.; Robb, M. A.; Cheeseman, J. R.; Zakrzewski, V. G.; Montgomery, J. A., Jr.; Stratmann, R. E.; Burant, J. C.; Dapprich, S.; Millam, J. M.; Daniels, A. D.; Kudin, K. N.; Strain, M. C.; Farkas, O.; Tomasi, J.; Barone, V.; Cossi, M.; Cammi, R.; Mennucci, B.; Pomelli, C.; Adamo, C.; Clifford, S.; Ochterski, J.; Petersson, G. A.; Ayala, P. Y.; Cui, Q.; Morokuma, K.; Rega, N.; Salvador, P.; Dannenberg, J. J.; Malick, D. K.; Rabuck, A. D.; Raghavachari, K.; Foresman, J. B.; Cioslowski, J.; Ortiz, J. V.; Baboul, A. G.; Stefanov, B. B.; Liu, G.; Liashenko, A.; Piskorz, P.; Komaromi,

- I.; Gomperts, R.; Martin, R. L.; Fox, D. J.; Keith, T.; Al-Laham, M. A.; Peng, C. Y.; Nanayakkara, A.; Challacombe, M.; Gill, P. M. W.; Johnson, B.; Chen, W.; Wong, M. W.; Andres, J. L.; Gonzalez, C.; Head-Gordon, M.; Replogle, E. S.; Pople, J. A. Gaussian, Inc., Pittsburgh, PA, 2002.
- (13) The corresponding 2-silyl-substituted complex was not available. According to our calculations, this compound is very strained and is 80 kJ/mol less stable than its 1-silyl-substituted congener. It seems plausible to us that the synthesis has failed due to this strain.
- (14) Wieser, U.; Schaper, F.; Brintzinger, H. H.; Mäkelä, N. I.; Knuuttila, H. R.; Leskelä, M. *Organometallics* **2002**, *21*, 541.
- (15) Mäkelä, N. I.; Knuuttila, H. R.; Linnolahti, M.; Pakkanen, T. A.; Leskelä, M. A. *Macromolecules* **2002**, *35*, 3395.
- (16) (a) van Beek, J. A. M.; Pieters, P. J. J.; van Tol, M. F. H. *Metallocenes '95*, Brussels, April 26–27, 1995. (b) Pieters, P. J. J.; van Beek, J. A. M.; van Tol, M. F. H. *Macromol. Rapid Commun.* **1995**, *16* (7), 463. (c) Coevoet, D.; Cramail, H.; Deffieux, A. *Macromol. Chem. Phys.* **1998**, *199*, 1459. (d) Pédetour, J.; Coevoet, D.; Cramail, H.; Deffieux, A. *Macromol. Chem. Phys.* **1999**, *200*, 1215. (e) Coevoet, D.; Cramail, H.; Deffieux, A.; Mladenov, C.; Pedetour, J.; Peruch, F. *Polym. Int.* **1999**, *48*, 257. (f) Wieser, U.; Brintzinger, H. H. In *Organometallic catalysts and olefin polymerization*; Blom, R., Follestad, A., Rytter, E., Tilset, M., Ystenes, M., Eds.; Springer-Verlag: Berlin, 2001; p 3. (g) Pédetour, J.; Cramail, H.; Deffieux, J. *Mol. Catal. A: Chem.* **2001**, *174*, 81. (h) Pédetour, J.; Cramail, H.; Deffieux, J. *Mol. Catal. A: Chem.* **2001**, *176*, 87.
- (17) Barsties, E.; Schaible, S.; Prosenc, M.-H.; Rief, U.; Röhl, W.; Weyand, O.; Dorer, B.; Brintzinger, H.-H. *J. Organomet. Chem.* **1996**, *520*, 63.
- (18) Piccolrovazzi, N.; Pino, P.; Consiglio, G.; Sironi, A.; Moret, M. *Organometallics*, **1990**, *9*, 3098.
- (19) Piemontesi, F.; Camurati, I.; Resconi, L.; Balboni, D.; Sironi, A.; Moret, M.; Zeigler, R.; Piccolrovazzi, N. *Organometallics* **1995**, *14*, 1256.
- (20) Linnolahti, M.; Pakkanen, T. A.; Leino, R.; Luttikhedde, H. J. G.; Wilén, C.-E.; Näsman, J. H. *Eur. J. Inorg. Chem.* **2001**, 2033.

MA034110C